Rev. Roum. Sci. Techn.– Électrotechn. et Énerg.
Vol. **62**, *2*, pp. 215–222, Bucarest, 2017

Génie biomédicale

ANALYSIS OF EYE IMAGE SEGMENTATION USED IN EYE TRACKING APPLICATIONS

ALEXANDRU PĂSĂRICĂ[1], RADU GABRIEL BOZOMITU[1], DANIELA TĂRNICERIU[1], GLADIOLA ANDRUSEAC[2], HARITON COSTIN[2, 3], CRISTIAN ROTARIU[2]

Key words: Eye tracking, Image segmentation, Assistive technology, Threshold selection.

This paper presents a comparison of different threshold-based selection methods, implemented and adapted for eye image segmentation. We used three subclasses of segmentation methods: fixed threshold segmentation (fixed threshold, quantitative threshold and cumulative distribution function method), global threshold segmentation (minimum error Kittler and characteristic separation), and local adaptive threshold (Bradley, Bernsen and Niblack methods). We compared the segmentation methods in order to determine their performances for video images and their suitability for eye tracking applications. In normal working situation using the eye tracking system we can use a global threshold value and in difficult conditions (different or fluctuating lighting) we can use a local adaptive threshold.

1. INTRODUCTION

Eye tracking application is a field of interest in recent research due to the improvement of the hardware used, mainly miniaturized and high resolution cameras and portable devices with high processing power (smartphones and tablets) [1]. These applications can be found in fields such as assistive technology for patients with neuro-motor disabilities [2], automotive industry as means of drowsiness assessment or automotive driving assistance [3] and data security or person identification based on eye tracking [4].

The main method, used to improve eye tracking applications in terms of increasing the precision and lowering the running time, is the image segmentation in order to highlight the pupil contour [5, 6].

Standard segmentation methods were implemented in order to analyze documents, thus the results obtained for eye images are not usable in eye tracking applications. The example in Fig. 1 presents the results obtained for the segmentation of eye images using the Otsu thresholding method [7]. These results cannot be used in an eye tracking application.

The purpose of this paper is to implement and adapt various threshold selection methods such as fixed threshold, quantitative threshold, minimum error threshold (Kittler method), integral image sum threshold (Bradley method), Bernsen method and Niblack method and compare them with a proposed method implemented specifically for eye image segmentation – the characteristics separation method.

2. EYE IMAGE SEGMENTATION USED IN EYE TRACKING APPLICATIONS

The experimental results were obtained by analyzing two databases.

The first dataset used for this analysis consists of 184 infrared (IR) images acquired in laboratory conditions (see Fig. 2). These images consist of different pupil positions (up/down, left/right) in order to observe the way the pupil shape changes from circular to elliptic, depending on the filming angle and gaze direction. The images were acquired using a modified USB camera with the resolution 640 × 480 pixels. We modified the camera by replacing the light source with LED lights and the camera objective was covered with an infrared glass filter. This does not influence the camera's technical parameters (resolution of 640 × 480 pixels and 30 frames per second acquisition rate). This allows us to benefit of the dark pupil technique [8] which is characterized by the fact that the cornea has a high degree of refraction of IR light, making the pupil the darkest region of the eye image. The camera is mounted on a frame from a pair of glasses. This assures that the relative distance between the eye and the camera does not vary by a high amount when used by different subjects.

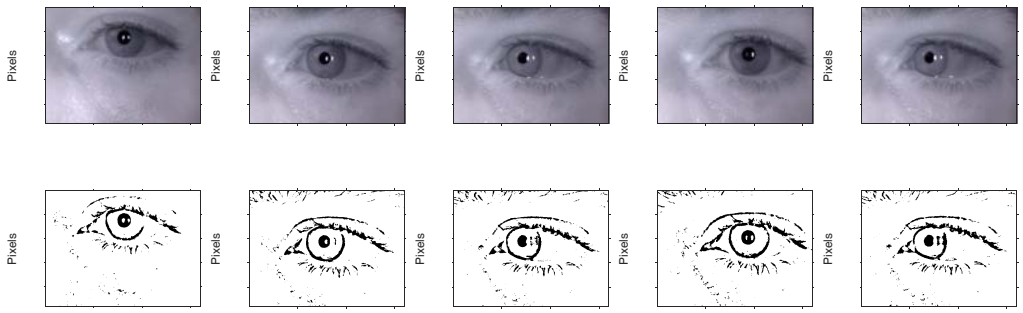

Fig. 1 – Results obtained with Otsu thresholding method.

[1] "Gheorghe Asachi" Technical University of Iasi, Faculty of Electronics, Telecommunications and Information Technology, E-mail: alexpasarica@gmail.com
[2] "Grigore T. Popa" University of Medicine and Pharmacy of Iasi, Faculty of Medical Bioengineering, E-mail: cristian.rotariu@umfiasi.ro
[3] Institute of Computer Science of Romanian Academy, Iasi Branch

The second dataset consists of 410 IR eye images from a publicly available database (CASIA-Iris-Lamp) [9]. The database contains a much larger number of images (16212), but for this application we have selected only 10 images from the each of the first 41 subjects from the database. The main characteristic of these images is that the pupil position is central, if the subject is looking straight forward, but the illumination conditions are different between subjects.

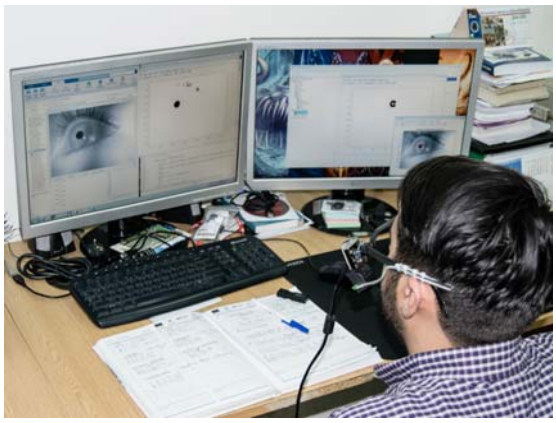

Fig. 2 – Experimental setup used for image acquisition.

The resolution for the images in this database is 640 × 480 pixels. In this case the camera was fixed and the subject would rest their chin on a support placed in front of the camera. The use of the two databases allows us to study both the influence of lighting and pupil position when trying to identify an adequate segmentation algorithm that can be used for real-time eye tracking applications.

Overall, for both databases, we determined experimentally that the number of pixels of the pupil image is never higher than 1% of the total number of pixels of the image. This value was determined by identifying the ideal pupil area for images in both datasets and obtaining the interval 0.3 %–0.8 %.

We preprocess each image by applying a 3 × 3 smoothing filter in order to remove salt and pepper noise due to singular dark pixels on white background in the eyelashes and eyebrows areas [10]. Another aspect that has to be taken into consideration is the presence of the corneal reflection. This can lead to low accuracy when analyzing certain images, so we remove it completely or partially after we apply the segmentation threshold by using pixel dilation followed by filling the gaps inside the contour (Fig. 3) [11]. This method cannot be used to remove corneal reflection situated on the edge of the pupil contour.

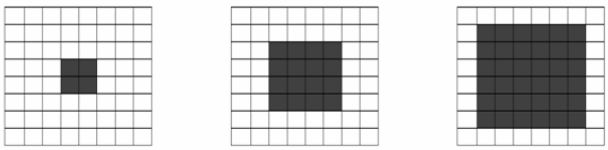

Fig. 3 – Simple example of pixel dilation
from the original image to dilation by one or two pixels.

2.1. EXPERIMENTALLY DETERMINED FIXED THRESHOLD

The fixed threshold selection is an efficient segmentation method, but it has the drawback that the acquired images can differ in terms of lighting and physiological parameters, leading to the necessity to readapt the threshold for each analysis [12]. We determined the optimal value by decreasing the threshold value from 0.5 to 0.1 on the normalized gray scale until we obtain the best segmentation results. The threshold value used for the analyzed datasets was 0.1 because this value allows for the best degree of separation between image components. Fig. 4 presents the segmentation results for an image taken as example, with the accuracy (Acc) obtained for that image shown in brackets. The accuracy value is obtained using formula (15).

2.2 FIXED QUANTITATIVE THRESHOLD

The fixed quantitative threshold selection method relies on identifying the number of pixels that correspond to the pupil contour as a percentage of the total number of image pixels [13]. The total number of pixels is defined as:

$$\text{Total\_pixels} = m \times n, \tag{1}$$

where m and n represent the camera resolution (m = 640 and n = 480). The approximate size of the pupil can be found in a 85 × 85 pixels window which represents 0.3 % of the total number of pixels in the 640 × 480 image. The value 0.5 % is the best compromise in order to retain as much as possible of the pupil image and not obtain artifacts due to eyelashes and eyebrows. We determine the number of pixels that correspond to the pupil contour by using the threshold value t = 0.5 % :

$$\text{Pupil\_pixels} = \text{Total\_pixels} \times t, \tag{2}$$

where Pupil_pixels represents the number of pixels that correspond to the pupil contour.

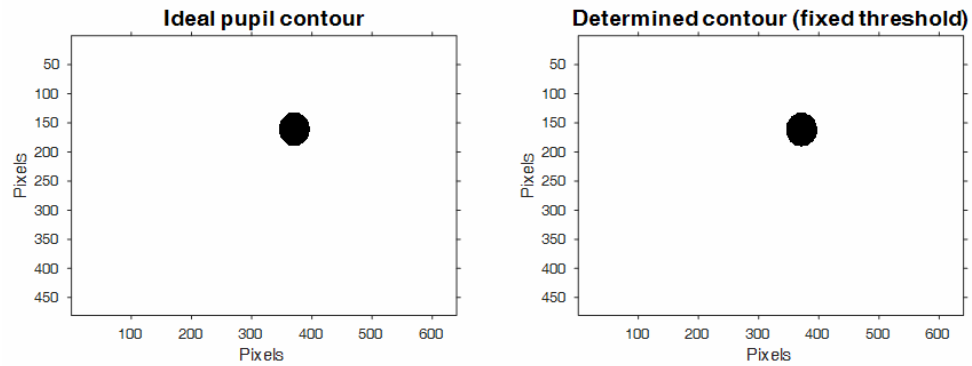

Fig. 4 – Comparison between the real pupil contour and the contour
obtained by applying a fixed threshold of 0.1 (Acc = 92.61 %).

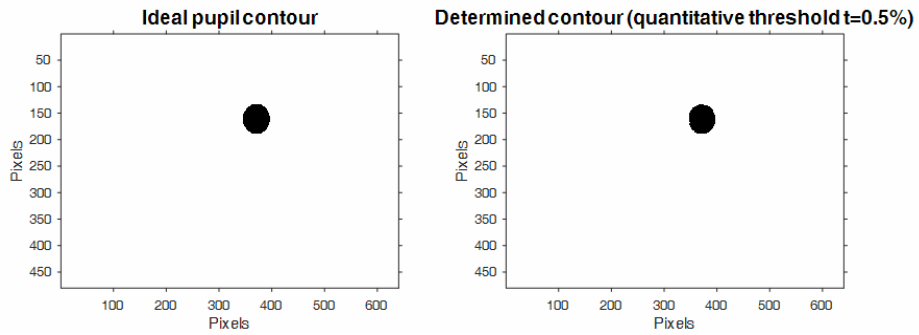

Fig. 5 – Comparison between the ideal contour and the contour determined by applying a quantitative threshold $t = 0.5$ % (Acc = 94.64 %).

By adding the number of pixels for the lower values of the intensities on the gray scale we obtain a sum larger than the Pupil_pixels value. The index for which this value is surpassed represents the threshold value. Fig. 5 represents the segmentation results for the threshold value $t = 0.5\%$.

2.3. CDF THRESHOLD

The cumulative distribution function (CDF) is a tool for the analysis of the image histogram in order to determine the darkest area of the eye image [14]. The filtered image is used to determine the CDF based on the following formula:

$$\mathrm{CDF}(r) = \sum_{w=0}^{r} p(w), \tag{3}$$

where $p(w)$ is the image histogram which represents the probability of the appearance of a gray value of intensity w and r is the gray intensity between [0; 255].

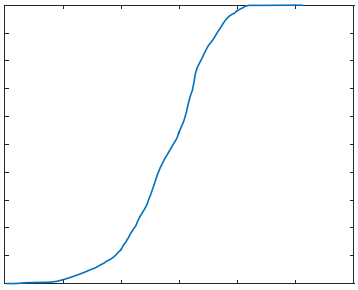

Fig. 6 –The CDF of the eye image histogram.

The CDF of the image histogram is presented in Fig. 6.

Based on the CDF values, we modify the pixel intensity values $I(x, y)$ as follows:

$$I(x,y) = \begin{cases} 255 \text{ if } \mathrm{CDF}(I(x,y)) < T \\ 0 \text{ if } \mathrm{CDF}(I(x,y)) \geq T \end{cases}, \tag{4}$$

where T is the threshold value of 0.004, used to analyze the $\mathrm{CDF}(I(x, y))$, which represents the normalized cumulative distribution function.

The algorithm relies on identifying the minimum gray intensity pixels (MIP) which are the dark pixels in the image that correspond to the pupil. There is a high probability that the MIP can be part of different areas other than the pupil (eyebrows or eyelashes), so we compare the MIP value to the average value of the intensity of the pixels in a 10×10 window centered on the analyzed MIP. The comparison between the determined contour using this method and the ideal pupil contour is presented in Fig. 7 [15].

2.4. CHARACTERISTICS SEPARATION METHOD

The characteristics separation method relies on the fact that the pixels that correspond to the pupil contour are the darkest pixels in the image. We apply the algorithm for the gray scale interval 0 to 125, this interval being sufficient to separate the pupil contour from other components in the image.

We first compute the image histogram for the selected interval of the gray scale. We then apply a smoothing filter with a moving window with the length equal to 5% of the total vector length. We apply the implemented peak detection algorithm to the smooth histogram vector elements that relies on determining the first derivative of the signal in order to obtain the peak values [16] (Fig. 8). We define the threshold value that is represented by the index of the minimum value between the first identified peak (which corresponds to the dark pixels of the pupil contour) and the end of the analyzed gray scale interval (gray scale intensity 125), obtaining the image segmentation presented in Fig. 9.

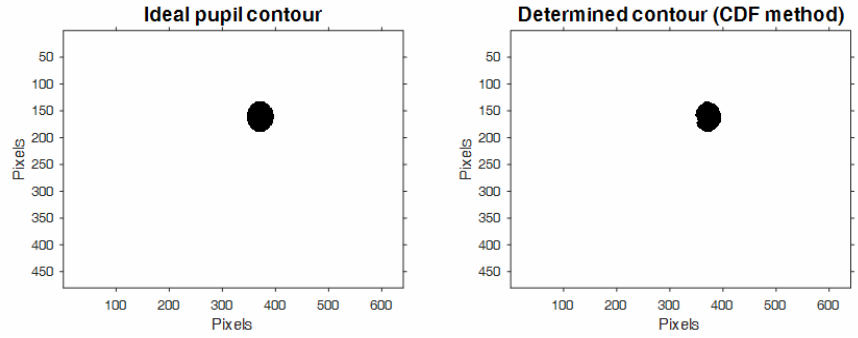

Fig. 7 – Comparison between the ideal contour and the determined contour using the CDF method (Acc = 90.95 %).

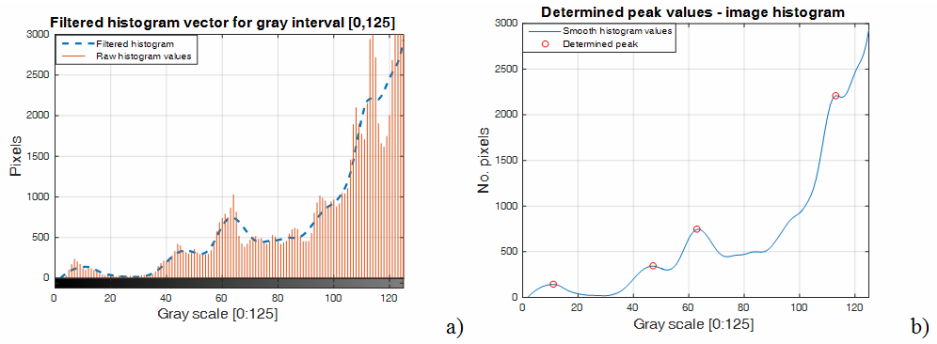

Fig. 8 –a) Image histogram raw and filtered data; b) determined peak values.

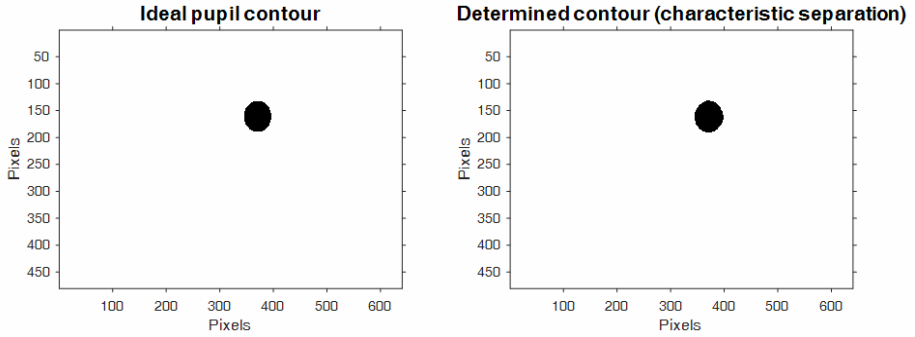

Fig. 9 – Results obtained for the characteristic separation method (Acc = 87.56 %).

2.5. KITTLER MINIMUM ERROR

The Kittler minimum error selection threshold consists in analyzing every gray scale intensity value t over the selected interval of the gray scale. The interval was selected between 0 and 95 [17] due to the fact that the pixels that correspond to the pupil are the darkest pixels in the image. We determine the bimodal histograms for two different classes represented by the subintervals 0 to t and $t + 1$ to 95, where t takes values from 0 to 95. The two histograms represent two different classes of pixels. We determine the number of pixels in each class for each gray scale intensity, and the standard deviation of each class using the following formulas:

$$\sigma_1 = \sqrt{\left[\sum_{i=1}^{t}\left(P_i \times Gs_i - M_1\right)^2\right] / C_1}\ , \tag{5}$$

where σ_1 is the standard deviation of the first class from 0 to t, P_i represents the number of pixels of intensity i, Gs_i intensity i on the gray scale, M_1 the mean value of the pixels intensity and C_1 the total number of pixels in the first class.

$$\sigma_2 = \sqrt{\left[\sum_{i=1}^{t}\left(P_i \times Gs_i - M_2\right)^2\right] / C_2}\ , \tag{6}$$

where σ_2 is the standard deviation of the second class for the interval t +1 to 95, P_i represents the number of pixels of intensity i, Gs_i the i value of the intensity of the gray scale, M_2 the mean value of the pixel intensities in the second class and C_2 the total number of pixels in the second class.

Based on the standard deviation values we determine the selection criterion of the threshold value based on [18]:

$$\begin{aligned} S(t) = 1 + 2 \times \left(C_1 \times \log\left(\sigma_1\right) + C_2 \times \log\left(\sigma_2\right)\right) - \ldots \\ - 2 \times \left(C_1 \times \log\left(C_1\right) + C_2 \times \log\left(C_2\right)\right). \end{aligned} \tag{7}$$

The minimum value of the elements of the selection criterion vector $S(t)$ represents the threshold value used to analyze images in the dataset. An example is given in Fig. 10.

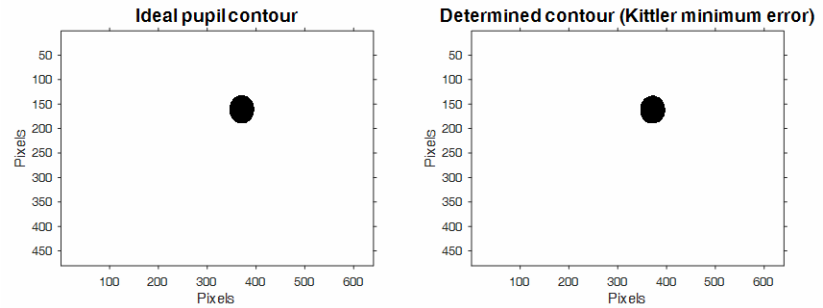

Fig. 10 – Comparison between the real pupil contour and the results obtained by using the Kittler minimum error (Acc = 94.72 %).

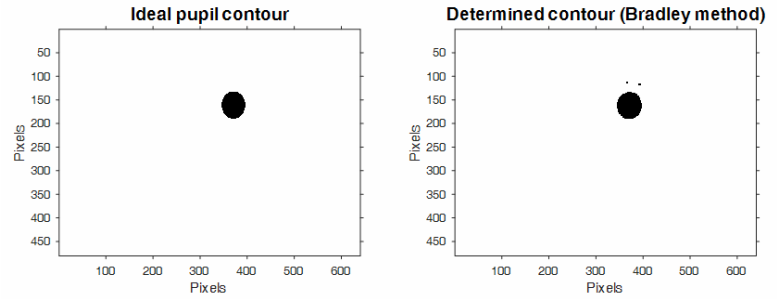

Fig. 11 – Comparison between the real pupil contour and the determined contour using the Bradley method for integral image sum (Acc = 92.23 %).

2.6. INTEGRAL IMAGE SUM (BRADLEY METHOD)

The integral image sum method is realized by determining the sum of the intensities of the pixels situated above and to the left of each pixel of the analyzed image [19]. Thus, for a pixel or point $A(x, y)$ we determine the integral sum as follows:

$$g(x,y)=\sum_{i=1}^{x}\sum_{j=1}^{y}I(i,j), \tag{8}$$

where $g(x, y)$ is the integral sum for a point $A(x, y)$ and I is the analyzed image.

Implementing this method and adapting it to eye image segmentation requires us to analyze a moving window with the dimension that approximates the size of the pupil. We select this as a wxw window ($w = 50$ pixels). For each window we determine a local integral sum $S(x, y)$ [20]. The local sum is determined as follows:

$$S(x,y)=\sum_{i=x-c}^{x+c}\sum_{j=y-c}^{y+c}I(i,j), \tag{9}$$

where $c=(w-1)/2$.

The integral image sum method segmentation example is presented in Fig. 11.

2.7 BERNSEN METHOD

This method is used to determine a local adaptive threshold value of an image window with the size wxw, where w is selected as 75 pixels. The method consists of computing the local minimum and maximum of the analyzed window, and then determining the local threshold value as the average [21]:

$$T_{Bernsen}=\left(f_{\max}+f_{\min}\right)/2, \tag{10}$$

where $T_{Bernsen}$ is the local threshold value, $f_{\max}$ is the local maximum value and $f_{\min}$ is the local minimum value (Fig. 12).

The pixels are classified as pupil pixels or background pixels based on the local threshold value and the variance which is determined using the formula:

$$\mathrm{Var}_{\mathrm{Bernsen}}=f_{\max}-f_{\min}, \tag{11}$$

where $\mathrm{Var}_{\mathrm{Bernsen}}$ is the variance and $f_{\max}$ and $f_{\min}$ have the same meaning as the previous formula.

The pupil pixel classification is verified by comparing the threshold value to the variance based on the following conditions [22]:

$$P_i=\begin{cases}0, \text{ if } \mathrm{I}\le T_{Bernsen} \text{ and } \mathrm{Var}_{\mathrm{Bernsen}} > T_{Bernsen}\\ 1, \text{ if } \mathrm{I} > T_{Bernsen} \text{ and } \mathrm{Var}_{\mathrm{Bernsen}} \le T_{Bernsen}\end{cases}, \tag{12}$$

where P_i is the analyzed pixel i and I is the pixel intensity on the normalized gray scale. The example for eye image segmentation using Bernsen method is presented in Fig. 12.

2.8. NIBLACK METHOD

The Niblack threshold method relies on determining the local mean and the standard deviation of a sliding window of dimensions $w \times w$ [23]. For this analysis we use a window of $w = 85$ pixels, which approximates the pupil size. The threshold is determined using the formula:

$$T_{Niblack}=\mathrm{mean}(I[w,w])+k\times\delta(I[w,w]), \tag{13}$$

where $T_{Niblack}$ is the local threshold value of the window $I[w, w]$, δ is the standard deviation of the pixels in the same window and k is a constant that is used to scale the segmentation results towards the higher or lower spectrum of the normalized gray scale. For this application $k = 0.9$.

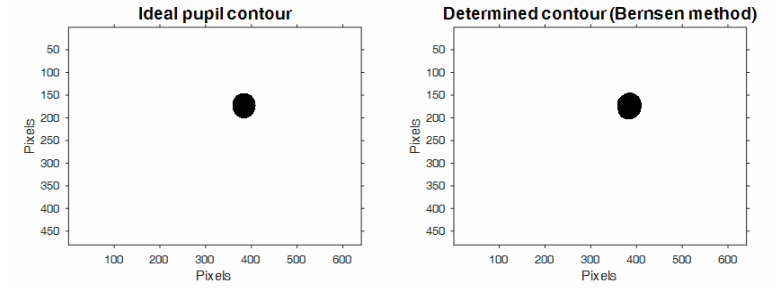

Fig. 12 – Comparison between the real pupil contour and the determined contour using the Bernsen method (Acc = 90.23 %).

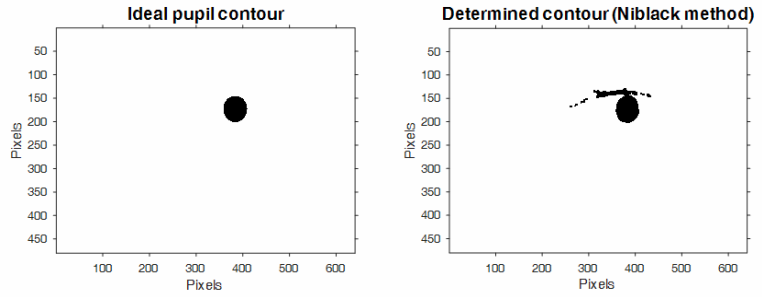

Fig. 13 – Comparison between the real pupil contour and the determined contour using the Niblack method (Acc = 77.89 %)

The standard deviation is determined using the formula:

$$\delta = \sqrt{\frac{1}{\mathrm{NP}} \sum \left(P_i - \mathrm{mean}\left(I\left[w, w \right] \right) \right)^2} , \qquad (14)$$

where NP represents the total number of pixels of the analyzed window, P_i is the gray scale intensity of the pixel i and the mean value is the same as in formula (13) [24].

The Niblack local threshold does not provide information about the global attributes of the image, thus an image with bad illumination will not be analyzed effectively (Fig. 13). Another aspect that has to be taken into consideration is the k value which has to be variable in order to obtain good results for images with a high variation of gray scale values [25].

3. EXPERIMENTAL RESULTS

The first dataset (DB1) consists of 184 IR (infrared) images with the resolution of 640 × 480, and these images were used to assess the performances of the image segmentation methods. The reference for this analysis is represented by the ideal pupil contour determined by manually analyzing the used images. The performance is measured as the accuracy with which we determine the pupil contour in the image by using each method implemented.

The second dataset (DB2) is a selection of 410 IR images from the publicly available database Casia-Iris–Lamp. The reference is obtained similarly to the first dataset.

We classify the image pixels as follows:

Pupil pixels – dark inner pixels that correspond to the pupil contour. The correctly determined pixels are named correct_pupil_pixels (CPP) and the pixels determined as pupil pixels that are in fact background pixels are named False_pupil_pixels (FPP).

Background pixels – pixels that are part of the image background and characterized as light pixels of the binary image. Similarly to the pupil pixels, we classify these as Correct_background_pixels (correctly identified background pixels – CBP) and False_background_pixels (background pixels identified as pupil pixels - FBP).

We determine the overall accuracy of each implemented method by using the following formula [26, 27]:

$$\mathrm{Acc}[\%] = \frac{\mathrm{CPP}}{\mathrm{CPP} + \mathrm{FPP} + \mathrm{FBP}} \times 100 . \qquad (15)$$

Table 1 presents the accuracy results obtained, compared by means of average values and standard deviation of the results over the entire datasets for the confidence interval (CI) of 95 %.

Table 1

Accuracy results of the implemented segmentation methods for the two datasets (DB1 and DB2)

Method	**Avg Acc % DB1**	**Std DB1(CI = 95%)**	**Avg Acc % DB2**	**Std DB2 (CI = 95%)**
Fixed threshold	83.41	6.78	79.17	13.98
Quantitative t = 0.5 %	76.04	16.24	88.59	6.51
CDF	75.87	9.22	56.54	21.46
Characteristic separation	80.94	6.19	80.86	24.59
Minimum error Kittler	84.77	17.12	83.87	22.02
Integral sum Bradley	82.42	6.71	88.96	6.54
Bernsen threshold	81.92	5.84	85.94	19.43
Niblack threshold	64.87	12.23	29.86	27.21

Figures 14 and 15 and the accuracy results presented in Table 1 demonstrate the fact that the performances of the segmentation methods are influenced by the direction of the eye gaze and the angle on which the camera is placed. The pupil shape varies from circular to elliptic when the gaze changes direction to left/right or up/down (DB1). The different type of illumination can also influence these results (DB2).

4. CONCLUSIONS

The segmentation methods presented in this paper have different performances based on mean accuracy and standard deviation of this parameter for the analyzed datasets of images. This points towards the fact that the algorithms suitable for a real time eye tracking application are the characteristic separation method, the Bradley and Bernsen methods which are adaptive and robust threshold selection methods.

The methods implemented can be divided into subclasses. The first subclass is represented by fixed threshold using the CDF method and the quantitative method that rely on determining a threshold value that will be used to determine the pupil contour. For the CDF method the threshold value used is T = 0.004. For the quantitative method the percentage of pixels that correspond to the pupil is selected as p = 0.5 %. The threshold values can be selected in a calibration stage for a real time eye tracking application, but overall their performances do not indicate that they are suited for such applications.

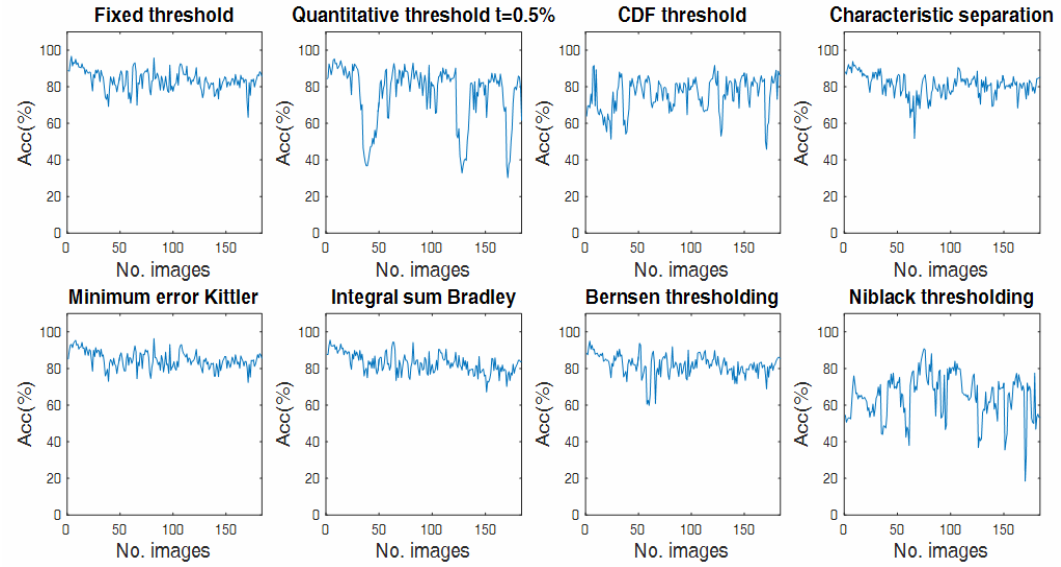

Fig. 14 – Comparison between methods in terms of accuracy (first database).

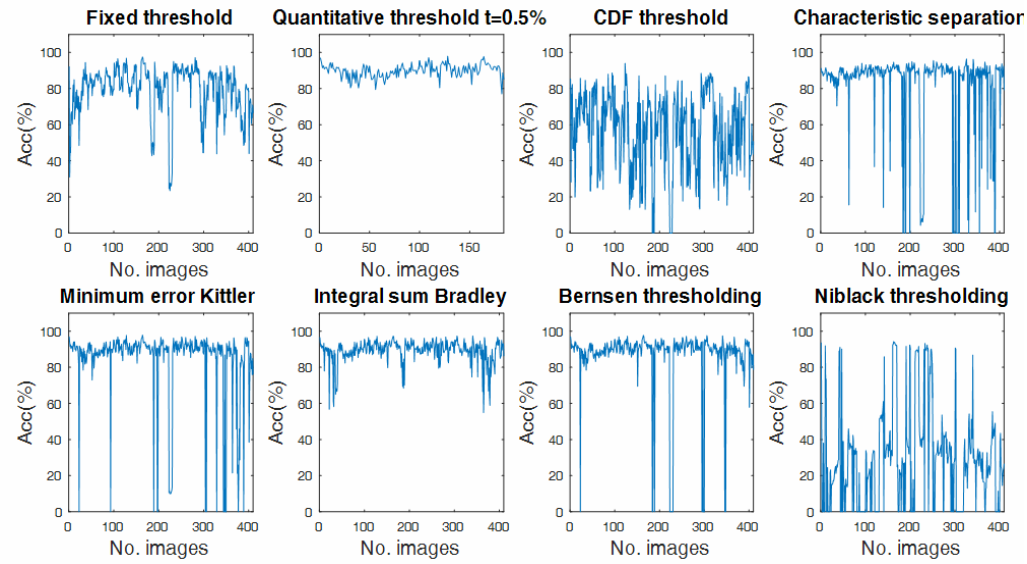

Fig. 15 – Comparison between methods in terms of accuracy (second database).

The second subclass consists in the analysis of the image histogram in order to determine a global threshold value. The methods in this subclass are the characteristic separation method and the Kittler minimum error method. Both these methods have accuracy results over 80% for both analyzed databases. The first method determines the minimum histogram element value after the first peak value that corresponds to the eye pupil. The Kittler method is best suited for bimodal histograms, which present a single minimum value. In order to obtain good results using this method we have to approximate the image histogram with a bimodal histogram by reducing the gray scale interval to a suitable value. In our analysis this value is 95 gray intensities.

The third subclass is represented by the local adaptive thresholding methods of integral image sum Bradley, Bernsen and Niblack. Of these three methods, the Bernsen and Bradley ones have the best performances with accuracy over 80% and low standard deviation values for both databases analyzed. The third method, Niblack, does not have good results, we mean less than 65 % accuracy, because the k value has to be variable for images with a high variation of gray scale values.

Overall, the segmentation methods best suited for real time eye tracking application based on the results obtained are the characteristic separation method for normal situations due to the lower runtime for each frame and the integral sum Bradley method for situations with fluctuating lighting, with the drawback of a higher runtime.

ACKNOWLEDGEMENTS

The work has been carried out within the program Joint Applied Research Projects, funded by the Romanian National Authority for Scientific Research (MEN – UEFISCDI), contract PN-II-PT-PCCA-2013-4-0761, no. 21/2014, SIACT.

This work was also supported by the project "Remote Monitoring of Physiological Parameters to Improve the Prediction of Fetal Outcome", financed by Grigore T. Popa University of Medicine and Pharmacy, Iasi, Romania, Contract No. 31592/23.12.2015.

Received on September 10, 2016

REFERENCES

1. C. Pino, I. Kavasidis, *Improving mobile device interaction by eye tracking analysis*, Computer Science and Information Systems (FedCSIS), Wroclaw, Poland, 2012, pp. 1199–1202.
2. R.G. Bozomitu, A. Pasarica, V. Cehan, R.G. Lupu, C. Rotariu, E. Coca, *Eye Tracking System Implementation based on Circular Hough Transform Algorithm*, IEEE International Conference on E-Health and Bioengineering (EHB), Iasi, Romania, 2015.
3. M.S. Devi, P.R. Bajaj, *Driver Fatigue Detection based on Eye Tracking*, First International Conference on Emerging trends in Engineering and Technology (ICETET), Nagpur, India, 2008, pp. 649–652.
4. R. Chappell, *System and Method for Eye Tracking Authentication*, International Patent Application, Publication Number: US20150227735 A1, 2015.
5. W. Sankowski, K. Grabowski, M. Napieralska, M. Zubert, A. Napieralski, *Reliable algorithm for iris segmentation in eye images*, Image and Vision Computing, **28**, pp. 231–237, 2010.
6. D. Cho, K.R. Park, D.W. Rhee, Y. Kim, *Pupil Localization for Iris Recognition in Mobile Phones*, 7th Acis International Conference on Software Engineering, Artificial Intelligence, Networking, and Parallel/Distributed Computing (SNPD), 2006, pp. 197–201.
7. N. Otsu, *An automatic threshold selection method based on discriminate and least squares criteria*, Denshi Tsushin Gakkai Ronbunshi, **63**, pp. 349–356, 1979.
8. D. Li, D. Winfield, D.J. Parkhurst, *Starburst: A hybrid algorithm for video-based eye tracking combining feature-based and model-based approaches*, Human Computer Interaction Program, Iowa State University, Ames, Iowa, 50010,University Science, 1989.
9. http://biometrics.idealtest.org/, Casia-Iris-Lamp
10. T. Huang, G. Yang, G. Tang, *A Fast Two-dimensional Median Filtering Algorithm*, IEEE Transactions on Acoustic, **27**, *1*, pp. 13–18, 1979.
11. W. Aydi, N. Masmoudi, L. Kamoun, *New Corneal Reflection Removal Method Used in Iris Recognition System*, International Journal of Electrical, Energetic, Electronic and Communication Engineering, **5**, *5*, pp. 697–701, 2011.
12. T.R. Singh, S. Roy, O.I. Singh, T. Sinam, K.M. Singh, *A new Local Adaptive Thresholding Technique in Binarization*, International Journal of Computer Science (IJCSI), **8**, *2*, pp. 271–277, 2011.
13. Y.J. Zhang, J.J. Gerbrands, *Objective and quantitative segmentation evaluation and comparison*, Signal processing, **39**, *1*, pp. 43–54, 1994.
14. H. Lee, *Method and Circuit for Extracting Histogram and Cumulative Distribution Function for Image Enhancement Apparatus*, Google Patents, 2001.
15. S.A. Durai, E.A. Saro, *Image Compression with Back-Propagation Neural Network using Cumulative Distribution Function*, World Academy of Science, Engineering and Technology, **17**, pp. 60–64, 2006.
16. M.I. Sezan, *A Peak Detection Algorithm and Its Application to Histogram-based Image Data Reduction*, Computer Vision, Graphics and Image Processing, **49**, *1*, pp. 36–51, 1990.
17. J. Kittler, J. Illingworth, *Minimum Error Thresholding*, Pattern Recognition, **19**, *1*, pp. 41–47, 1986.
18. Y. Zou, L. Fang, F. Dong, B. Lei, S. Sun, T. Jiang, P. Chen, *Median-based Thresholding, Minimum Error Thresholding, and Their Relationship with Histogram-based Image Similarity*, Sixth International Conference on Digital Image Processing (ICDIP), Athens, Greece, April 2014.
19. D. Bradley, G. Roth, *Adaptive Thresholding using the Integral Image*, Journal of Graphics Tools, **12**, *2*, pp. 13–21, 2007.
20. M. Bulea, *Image Processing and Pattern Recognition – Theory and Applications*, Editura Academiei Române, Bucharest, 2003, pp. 115–119.
21. M. Nandy, S. Saha, *An Analytical Study of Different Document Image Binarization Methods*, IEEE National Conference on Computing and Communication Systems (COCOSYS), India, Burdwan, 2009, pp. 71–75.
22. J. Bernsen, *Dynamic Thresholding of Gray Level Images*, Proceedings of the 8th International Conference on Pattern Recognition, Paris, 1986, pp. 1251–1255.
23. N. Bin Rais, M.S. Hanif, I.A. Taj, *Adaptive Thresholding Technique for Document Image Analysis*, Proceedings of 8th International Multitopic Conference (INMIC), 2004, pp. 61–66.
24. W. Niblack, *An Introduction to Digital Image Processing*, Prentice Hall, Englewood Cliffs, 1986.
25. R.G. Bozomitu, *Communication techniques based on eye gaze detection used in assistive technology*, Univ. Politehnica, Iasi, Romania, 2016.
26. A. Idrayan, *Medical Biostatistics*, Third Edition, Chapman & Hall CRC Press, 2012, pp. 280–283.
27. A. Pasarica, R.G. Bozomitu, O.D. Eva, D. Tarniceriu, C. Rotariu, *Analysis of Different threshold Selection Methods for Eye image Segmentation used in Eye Tracking Applications*, 13th International Conference on Development and Application Systems, Suceava, Romania, 2016, pp. 299–302.